

# EARLY LASING AT LCLS AND ITS IMPLICATIONS FOR FUTURE CAVITY-BASED XFELS

M. D. Balcazar\*, R. Margraf-O’Neal, J. Tang, A. Lutman, T. Maxwell,  
T. Sato, Z. Huang, D. Zhu, A. Halavanau  
SLAC National Accelerator Laboratory, Menlo Park, CA, United States

## Abstract

The Cavity-based XFEL is a future x-ray photon source under intense development at SLAC. It is considered to be a path towards full 3D coherence at angstrom wavelength, delivering another 2-3 orders of magnitude increase in source brightness compared to current XFELs configurations. One of the first goals of the project is to demonstrate the regenerative amplification by returning and amplifying the seed pulse from 7 LCLS hard X-ray undulators with a rectangular crystal cavity. In this paper, we report on the recent measurement of early stage XFEL lasing characteristics at 9.831 keV photon energy by using 7 LCLS HXUs under e-beam conditions close to those chosen for the first phase of CBXFEL gain demonstration.

## INTRODUCTION

In the realm of X-ray Free Electron Lasers (XFELs) the principles of seeding have been developed and are an active area of R&D. Particularly at LCLS, a hard X-ray self-seeding technique [1] has been successfully demonstrated and implemented for users utility. The integration of self-seeding techniques in XFELs not only revolutionizes the coherence properties of the emitted radiation but also enables new groundbreaking experiments. The self-seeding techniques also serve as an stepping stone into the next future light sources, including the Cavity-Based X-ray Free Electron Laser (CBXFEL) project [2-7].

The CBXFEL utilizes Bragg crystal optics to form a *resonant* cavity, in which the initial XFEL radiation pulse coherently interacts with the next fresh electron bunch from the accelerator. Through this process the cavity output x-rays would present advanced coherence characteristics both transversely and longitudinally, while simultaneously amplifying the pulse via FEL gain. The CBXFEL project at SLAC will use the first seven Hard X-ray Undulators (HXUs) in the LCLS undulator hall to realize this concept.

The goal of this study is to verify if the output radiation characteristics of the first seven HXUs at LCLS is consistent with theoretically calculated values, based on a regenerative amplifier free-electron laser (XRAFEL) configuration. In particular, this experiment measures the average radiation intensity and flux of the pulse, as well as it employs a monochromator to measure the spectrum of the x-ray pulses. We operate at 9.831 keV photon energy, as it corresponds to the wavelength value relevant to the CBXFEL project.

## EXPERIMENT

### Setup

The experimental setup utilizes the hard X-ray beamline at LCLS and a ( $C^*(111)$ ) double crystal monochromator located downstream at the X-ray Pump-Probe (XPP) hutch as shown in Fig. 1. Initially Chicane 1 (Cell 13) in the HXU line was enabled at its full delay, followed by the first 8 HXUs in LCLS, while keeping downstream undulator gaps all open. The initial size of the X-ray beam is in the order of  $\sim 40 \mu\text{m}$ , and downstream, it is  $\sim 300 \mu\text{m}$ .

The HXU modules were then removed one by one and the XFEL gained was recorded using two detectors: Diode 1 (D1) upstream, looking at scattering from a Silicon Nitride target, and a second detector Diode 2 (D2) downstream at XPP after the monochromator.

The next measurement was taken by D2 while scanning the angle of the XPP monochromator monochromator crystal ( $C^*(111)$ ) in order to measure the average x-ray pulse spectrum from its reflection. Multiple scans were recorded by similarly starting with 8 HXUs and subsequently removing HXUs one by one downstream and measuring the change in the X-ray flux within a narrow band in the center of the spectrum recorded at the X-ray Pump Probe (XPP) hutch.

### Experimental Results

We first applied a filter to discriminate the shots with respect to their corresponding e-beam energy. A data subset was then obtained with those shots falling within a narrow 2 MeV band at the center of the electron beam spectrum. Next, utilizing 7 HXUs the mean pulse energy was recorded using the first diode detector D1, resulting in a mean of  $\sim 0.115 \mu\text{J}$  or  $7 \times 10^7$  photons/pulse for the average radiation brightness of the "pink" pulse centered at 9.831 keV.

The mean number of photons from removing each of the HXUs one by one starting from 8 total down to only 3 as shown in Fig. 2. The resulting behavior shows an exponential increase in mean "pink" pulse energy with increasing number of HXUs. A pedestal in the measurements is also recorded, corresponding to background of synchrotron radiation having approximately  $\sim 2 \times 10^7$  photons.

The second diode detector D2 used in the experiment, located downstream at the XPP hutch was utilized to measure the bandwidth of the monochromatic X-ray beam as a function of number of HXUs. Within this context, Fig. 3 displays these measurements, indicating a clear trend in the spectra both in their amplitude and width. For analysis purposes Gaussian curves were fitted for each case and their area was normalized to the value recorded by the first diode D1 per

\* mdbm@slac.stanford.edu

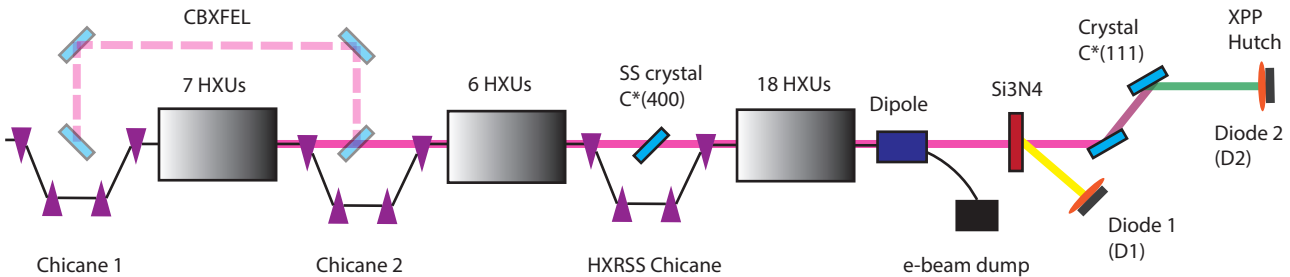


Figure 1: LCLS HXU beamline layout (not to scale) as of 2024: 7 tunable undulator sections are flanked by two electron beam chicanes for CBXFEL experiment, followed by 6 undulator sections, hard x-ray self-seeding (HXRSS) chicane and 18 more undulator sections. The resulting x-rays are intercepted with a  $\text{Si}_3\text{N}_4$  membrane for pulse intensity measurements, followed by a double crystal monochromator (DCM) and a photodiode detector.

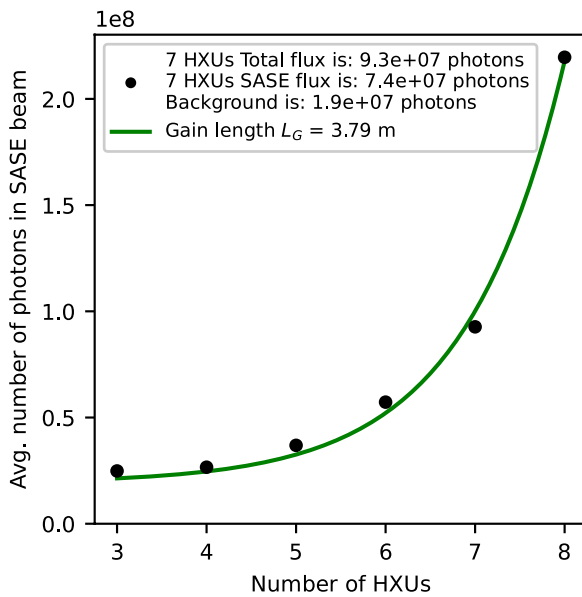


Figure 2: Average number of photons in a SASE beam as a function of number of HXUs. As more HXUs are inserted the photon numbers approaches an exponential fit with the gain length  $L_G = 3.79$  m as its characteristic parameter.

number of HXUs used, in order to convert the measurements from counts to  $\mu\text{J}$ , and subsequently number of photons. The relative FWHM bandwidth  $\Delta\omega/\omega$  of the fitted curve was subsequently measured based on the a number of HXUs as shown in Fig. 4.

Finally, the average number of photons was numerically calculated for a small 0.1 eV window at the center of the measured spectra, which corresponds to the CBXFEL cavity crystals operating bandwidth.

## DISCUSSION

In this case, the fitted parameters  $L_G = 3.79$  m in Fig. 2 correspond to the experimentally recovered 3D gain length for the early XFEL lasing. The Pierce parameter  $\rho$  (fundamental in 1D FEL theory) characterizes most properties of a high-gain FEL [3]. In this sense, an equation to calculate a theoretical estimate for the 1D Pierce parameter based on experimental conditions is given by,

$$\rho = \left[ \frac{I}{\gamma^3 I_A} \frac{\lambda_u^2}{2\pi\sigma_x\sigma_y} \frac{(K \times [JJ])^2}{32\pi} \right]^{1/3}. \quad (1)$$

Here  $I$  is the electron beam peak current,  $I_A$  is the Alfvén current,  $\gamma$  is the Lorentz boost factor,  $\lambda_u^2$  is the undulator wavelength,  $\sigma_{x,y}$  is the transverse RMS beam size (for a Gaussian distribution),  $K$  is the undulator strength parameter, and the term  $[JJ] = J_0(\xi) - J_1(\xi)$  is the subtraction from two Bessel functions when evaluated at  $\xi = K^2/2(2 + K^2)$ .

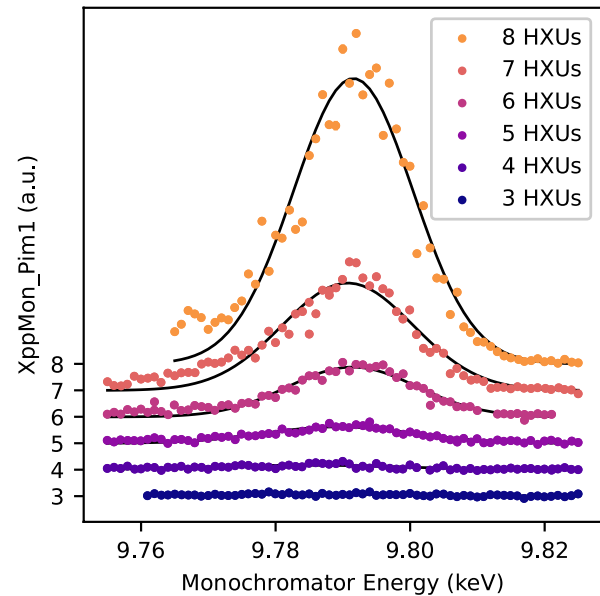


Figure 3: Average x-ray pulse spectra for different number of undulators, as measured using a DCM and performing a "rocking curve" scan by rotation the crystals in small angles and capturing the signal response in a diode.

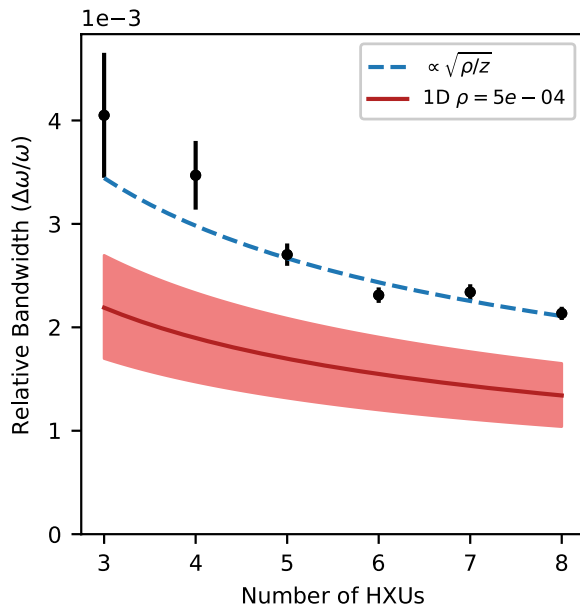


Figure 4: Relative average pulse bandwidth as a function of number of undulators, obtained by calculating the FWHM of the spectral measurements and dividing by the center frequency.

Using realistic experimental parameters in this study (see Table 1) leads to an estimate of  $\rho \approx 5 \times 10^{-4}$ .

Table 1: Summary Table of Parameters Used to Calculate the 1D Pierce Parameter

Parameter	Variable	Value
Electron beam energy	$E$	10.65 GeV
Electron beam peak current	$I$	4094 A
Lorentz factor	$\gamma$	20911
Alfven current	$I_A$	17000 A
Normalized sliced emittance	$\hat{\epsilon}_{x,y}$	$0.5 \times 10^{-6}$
Undulator period	$\lambda_u$	2.6 cm
Transverse RMS beam size	$\sigma_x, \sigma_y$	15 – 30 $\mu$ m
Undulator parameter	$K$	1.8

It is also possible to utilize the theoretically calculated Pierce parameter  $\rho$  and the undulator wavelength  $\lambda_u$  to calculate order-of-magnitude estimates of numbers with respect of the beam dynamics [9]. For instance, one expects the 1D gain length to be in the order of

$$L_{G0} \sim \frac{\lambda_u}{4\pi\sqrt{3}\rho}. \quad (2)$$

This expression for gain length, however, is not in 3D and does not include corrections for the energy spread, emittance and diffraction. In this sense, following the method described by Ming Xie [10, 11], one can find a corrected gain length fitting formula described as

$$L_G = L_{G0} (1 + \Delta). \quad (3)$$

Here the parameter  $\Delta$  is described in Ref. [9, 10]. We assume, for several reasons, the largest correction to come from the electron beam energy spread. Then, by calculating  $L_{G0}$  and utilizing the experimentally fitted gain length  $L_G = 3.79$  m it is possible to extract the deviation  $\Delta$ , and therefore an estimate for energy spread. Since  $L_G \approx L_{G0} [1 + (\sigma_\gamma/\rho)^2] \rightarrow \Delta \approx (\sigma_\gamma/\rho)^2$  then we obtain  $\sigma_\gamma * \gamma = \Delta E = 4.2$  MeV as calculated energy spread from the experimental measurements.

Finally, analyzing Fig. 4, 1D FEL theory predicts a dependence of the SASE radiation relative bandwidth (FWHM) as a function of the traveling distance  $z$ , such that

$$\frac{\Delta\omega}{\omega} = 2\sqrt{\ln(2)} \left( \frac{\sigma_\omega(z)}{\omega} \right). \quad (4)$$

Where the dependence of the relative RMS bandwidth on  $z$  is given by,

$$\frac{\sigma_\omega(z)}{\omega} = 3\sqrt{2}\rho \sqrt{\frac{L_{G0}}{z}}. \quad (5)$$

In this sense, the Pierce parameter  $\rho$  directly affects the dependence of relative bandwidth on number of HXUs since  $\Delta\omega/\omega \propto \sqrt{\rho/z}$ . Given that there is some uncertainty in the calculation of  $\rho$  there is also uncertainty in the calculated relative bandwidth. The comparison of theory with experimental measurements is shown in Fig. 4, in which it can be observed that the data indeed follows a similar dependence than the expected values. Albeit some uncertainties in the real 3D beam parameters such as differences in emittance, energy spread, beam size, and others, lead to overall slightly larger values of bandwidth experimentally than those predicted by theory.

## CONCLUSION

In summary, we have characterized early lasing process at the LCLS HXU line tuned at 9.831 keV photon energy. We have measured the number of SASE photons, and the projected average number of photons within the CBXFEL cavity bandwidth. The numbers presented in Table 2 corroborate our previous numerical simulations, thus confirming the feasibility of the upcoming CBXFEL experiment at LCLS.

Table 2: Summary table of average photon numbers obtained for the total flux in a SASE beam as well as for the flux in a small 0.1 eV bandwidth.

Average Quantity	Units	XRAFEL Pulse 1
Intensity, total	[ph/pulse]	$7.4 \times 10^7$
Intensity, mono	[ph/pulse]	$3.0 \times 10^5$
Flux, total	[ph/pulse/s]	$8.9 \times 10^9$
Flux, mono	[ph/pulse/s]	$3.6 \times 10^7$

## ACKNOWLEDGEMENTS

This work is supported by the U.S. Department of Energy Contract No. DE-AC02-76SF00515. We would like to thank Alberto Lutman, Zhirong Huang (SLAC) and the team of LCLS operators.

## REFERENCES

- [1] J. Amann *et al.*, “Demonstration of self-seeding in a hard X-ray free-electron laser”, *Nature Photonics*, vol. 6, no. 10, p. 693-698, Oct. 2012. doi:10.1038/NPHOTON.2012.180
- [2] K-J Kim, Y. Shvyd’ko, and S. Reiche, “A proposal for an X-ray free-electron laser oscillator with an energy-recovery Linac”, *Physical Review Letters*, vol. 100, no. 24, p. 244802, Jun. 2008. doi:10.1103/PhysRevLett.100.244802
- [3] Z. Huang and R. D. Ruth, “Fully coherent X-ray pulses from a regenerative-amplifier free-electron laser”, *Physical Review Letters*, vol. 96, no. 14, p. 144801, Apr. 2006. doi:10.1103/PhysRevLett.96.144801
- [4] G. Marcus *et al.*, “Regenerative amplification for a hard X-ray free-electron laser”, in *Proc. FEL’19*, Hamburg, Germany, Aug. 2019, pp. 118–121. doi:10.18429/JACoW-FEL2019-TUP032
- [5] W. Qin *et al.*, “Start-to-end simulations for an X-ray FEL oscillator at the LCLS-II and LCLS-II HE”, in *Proc. FEL’17*, Santa Fe, NM, USA, Aug. 2017, pp. 247–250. doi:10.18429/JACoW-FEL2017-TUC05
- [6] E. Allaria and G. De Ninno, “A step towards cavity-based X-ray free electron lasers”, *Nature Photonics*, vol. 17, no. 10, p. 841-842, Oct. 2023. doi:10.1038/s41566-023-01302-0
- [7] R. Margraf *et al.*, “Low-loss stable storage of 1.2 Å X-ray pulses in a 14 m Bragg cavity”, *Nature Photonics*, vol. 17, no. 10, p. 878-882, Oct. 2023. doi:10.1038/s41566-023-01267-0
- [8] K.J Kim, Z. Huang, and Ryan Lindberg, “Practical considerations and experimental results for high gain FELs”, in *Synchrotron radiation and free-electron lasers*, Cambridge University Press, Mar. 2017. doi:10.1017/9781316677377
- [9] C. Pellegrini, A. Marinelli, and S. Reiche, “The physics of X-ray free-electron lasers”, *Reviews of Modern Physics*, vol. 88, no. 1, p. 015006, Mar. 2016. doi:10.1103/RevModPhys.88.015006
- [10] M. Xie, “Exact and variational solutions of 3D eigenmodes in high gain FELs”, *Nuclear Instruments and Methods in Physics Research Section A: Accelerators, Spectrometers, Detectors and Associated Equipment*, vol. 445, no. 1-3, p. 59-66, May 2000. doi:10.1016/S0168-9002(00)00114-5
- [11] M. Xie, “Grand initial value problem of high gain free electron lasers”, *Nuclear Instruments and Methods in Physics Research Section A: Accelerators, Spectrometers, Detectors and Associated Equipment*, vol. 475, no. 1-3, p. 51-58, Dec. 2001. doi:10.1016/S0168-9002(01)01534-0